

## The GAPS Time-of-Flight Detector

---

### Sydney Feldman<sup>a,\*</sup> for the GAPS collaboration

<sup>a</sup>*Dept. of Physics and Astronomy, University of California  
Los Angeles, CA, 90095 USA*

*E-mail:* [sydneyfeldman@physics.ucla.edu](mailto:sydneyfeldman@physics.ucla.edu)

The General Antiparticle Spectrometer (GAPS) Antarctic long duration balloon mission is scheduled for launch during the austral summer of 2024-25. Its novel detection technique, based on exotic atom formation, excitation, and decay, is specifically designed for the detection of slow moving cosmic antiprotons and antideuterons. Such antinuclei are predicted by a wide variety of allowed dark matter models, as well as other astrophysical theories like primordial black holes.

There are two main components of the GAPS instrument: a large-area tracker and a surrounding time-of-flight system (TOF). The combination of these two systems allows GAPS to effectively differentiate between species of negatively-charged antinuclei and determine the energy deposition, velocity, and trajectory of particles interacting with the detector. This contribution will focus on the TOF, which determines the velocity of the incoming antiparticle and provides the trigger to the experiment. We will give an overview of the TOF detector, an explanation of relevant electronics, and a report on its construction and preliminary performance. The TOF is composed of 160 thin plastic scintillator paddles ranging in length from 1.5 to 1.8 meters. At each paddle end, signals from six silicon photomultipliers are combined to produce two copies of the resulting waveform: one to form the trigger and one for data readout. This design is optimized for low mass and fast data acquisition while still maintaining good light collection.

38th International Cosmic Ray Conference (ICRC2023)  
26 July - 3 August, 2023  
Nagoya, Japan



---

\*Speaker

## 1. Introduction and Science Background

The unknown nature of dark matter (DM) requires investigation with many different experimental strategies. Typically, DM experiments are one of four complementary types: accelerator searches, direct detection, indirect detection, or astrophysical probes. Each of these approaches are optimized for examining the problem of DM from different angles [1]. The General AntiParticle Spectrometer (GAPS) is an indirect detection experiment which targets cosmic ray (CR) antinuclei as a potential dark matter signature. While antiparticles are not themselves DM candidates, a wide range of existing dark matter models predict antinuclei as a product of DM annihilation or decay [2, 3].

For this reason, CR antinuclei hold important information about the question of dark matter. A few years ago, the interpretation of Alpha Magnetic Spectrometer (AMS-02) antiproton data resulted in a potential DM signal (e.g. [4]). However, further analysis [5, 6] reduced the significance of the finding. The difficulty in fully understanding and disentangling background antiprotons from a potential signal motivates the GAPS search for antideuterons.

In addition to extending the antiproton spectrum to lower energies, the GAPS experiment will search this energy range for a potential antideuteron flux. This is a particularly interesting search due to the uniquely low background from known astrophysical processes. According to conventional physics, cosmic ray antideuterons are produced only through interactions of primary CRs with the interstellar medium (ISM). The minimum energy of an incident particle required for this interaction to produce antideuterons is high, and due to energy conservation the resulting spectra of antideuterons (secondary CRs) are boosted to higher energies, with a very low flux predicted at kinetic energies below 0.5 GeV/n [3]. Theories of antideuteron production beyond the standard model are not constrained in the same way, because DM annihilation happens nearly at rest. For example, annihilation of WIMPs would produce an antideuteron flux significantly above conventional physics backgrounds at low energies.

GAPS is a long duration balloon experiment scheduled to launch from Antarctica during the austral summer of 2024-25. This contribution will focus on the (time-of-flight system (TOF), which determines the energy deposition, velocity, and trajectory of incoming CR particles and provides the trigger to the experiment.

## 2. The GAPS Instrument

The GAPS instrument is composed of two main detector components: a large area lithium-drifted silicon tracker (Si(Li)), and the time-of-flight detector (TOF) which surrounds it. Detection and particle identification are accomplished with the following novel technique:

When a negatively charged antiparticle enters the detector volume, it will first interact with and deposit energy in the TOF, which forms the trigger for the experiment. Then, it slows down and is captured by the tracker material, forming a matter-antimatter bound state. This state is extremely unstable, and the decay and annihilation of the exotic atom produces X-rays, pions, and protons which also deposit energy in the tracker and TOF. In particular, the energy of the X-rays are characteristic of the reduced mass of the exotic atom, and can therefore be used to determine the

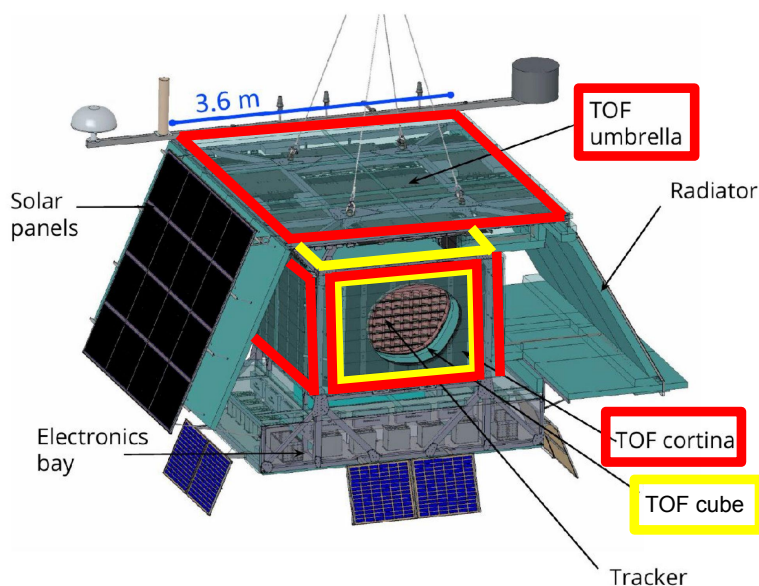


**Figure 1:** Overview of the GAPS instrument, with the outer TOF highlighted in red and the inner TOF highlighted in yellow.

charge-to-mass ratio of the captured particle. The stopping vertex can also be reconstructed from the tracks of annihilation products, leaving us with a full picture of the event [7].

This technique is optimized for the detection of CR antiparticles with less than 0.25 GeV per nucleon, where antiprotons have never been measured and antideuteron backgrounds are extremely low. This technique is less limited in aperture and mass compared to magnetic spectrometers. With over 7 m<sup>2</sup> of active Si(Li) detector area and 25 m<sup>2</sup> of TOF detector area, the geometric acceptance of GAPS is high, and yet it is light enough to be launched with a long-duration balloon.

## 2.1 Tracker

The tracker is composed of more than 1000 Si(Li) detectors, each of which is 10 cm in diameter, 2.5 mm thick, and segmented into eight strips. Four of the detectors are grouped together to form a module, which uses an Application Specific Integrated Circuit (ASIC) with 32 channels to provide power and read out data [8]. The modules are arranged in 7 layers with six rows of six modules.

The Si(Li) acts as both a target nucleus for the capture of a negatively charged antiparticle, and as an X-ray detector with a resolution of 4 keV FWHM in the relevant energy range [9]. The operational range of the tracker is around  $-35^{\circ}$  Celsius, which is accomplished with a passive oscillating heat pipe thermal system [10].

## 2.2 Time-of-Flight Detector (TOF)

The time-of-flight detector (TOF) is composed of 160 long, thin plastic scintillator paddles ranging in length from 1.5 to 1.8 meters. The paddles are arranged with a slight overlap between adjacent paddles into an inner TOF (the cube, closely surrounding the tracker on all six sides) and the outer TOF (a second layer on top of the cube, called the umbrella, and around the four sides,

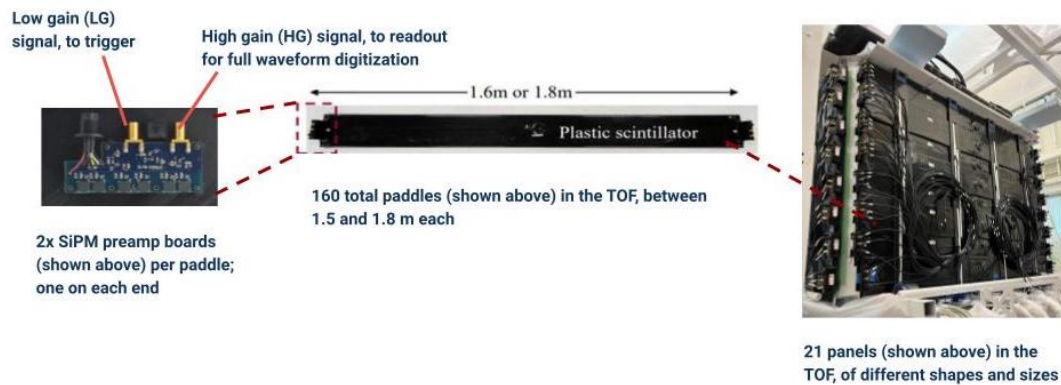


**Figure 2:** A SiPM preamp, fully wrapped paddle, and mounted TOF panel.

called the cortina). See Figure 1 for a diagram of the experiment with the inner and outer TOFs labeled, and Figure 2 for photos of a TOF paddle and panel.

This arrangement is designed to provide maximum coverage for events stopping in the tracker. The TOF is also used to track the out-going annihilation products, which is helpful for particle identification.

### 3. TOF Construction

The material which comprises the TOF detector area is Eljen EJ-200 general use plastic scintillator. The scintillator was machined by Eljen to have a width of 16 cm, a thickness of 6.35 mm, and lengths varying from 1.5 to 1.8 m. The paddles were wrapped first in aluminum foil and then vinyl blackout material in order to achieve good internal reflection and light-tightness. A small opening was left at the center of the paddle, where a venting tube was inserted in order to allow for outgassing and pressure changes without damage to the wrapping.

The scintillator light output is collected and readout by Silicon photomultipliers (SiPMs). Six SiPMs are attached to each side of a paddle, which connect to a preamplifier board. Aluminum enclosures were built around each SiPM preamp board, and each board was tested to confirm that all six of the SiPMs had a relatively similar gain. For this test, an LED, step motor, and darkbox was used to collect data for 1000 LED flashes in front of each of the six SiPMs. Although the results did not provide an exact gain value, they clearly indicated when one of the SiPMs was non-functional, and they also showed the spread in the response of performance across SiPMs (which was determined to be a measure of the relative gain). Examples of acceptable and unacceptable SiPM responses, depicted with distributions of integrated charge per event, are shown in Figure 3.

When a preamp was shown to have an even response to light pulses across all six SiPMs, it was coupled to the end of a paddle using silicon optical interfaces and optical cement. Two preamp boards were adhered to each paddle. An intricate wrapping procedure was then performed to make the nontrivial geometry of the preamp enclosure light-tight. To confirm light-tightness, the paddle was thoroughly inspected using a flashlight, with a specific focus on the edges of the wrapping material and any difficult corners.

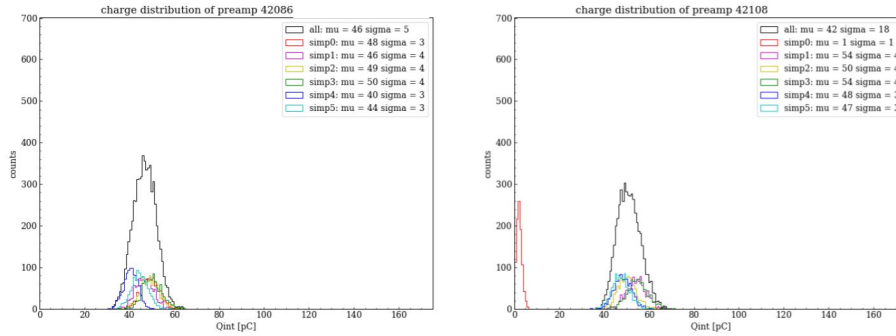


**Figure 3:** Left: Distribution of integrated charge per event for 6000 events with a well-performing SiPM preamp. Right: Distribution of integrated charge per event for an unacceptable SiPM preamp. Note that one SiPM of the six in the preamp did not have a response to the LED pulse.

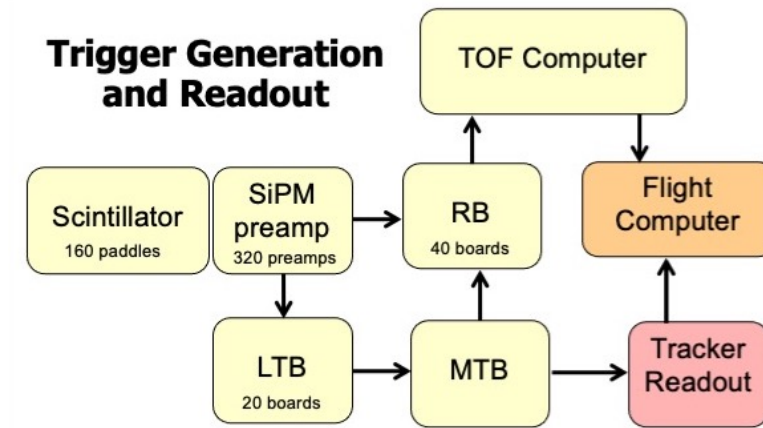


**Figure 4:** A diagram of the signal pathway for the GAPS trigger generation and readout.

Then, muon calibration data were taken for each paddle to verify that the gains were balanced between paddle ends; this ensures uniform illumination of the paddle. Finally, the paddles were strapped to carbon fiber panels which mounted to the gondola frame of the experiment. The panels are arranged into the inner TOF, which is a *cube* that closely encloses the tracker from all six sides, and the outer TOF, which is composed of the *umbrella* (a single layer above the cube top) and the *cortina* (an additional layer around the four cube sides); see Figure 1.

Using the time difference between signals from the same paddle along with the known speed of light in the scintillator material, we are able to determine where along the paddle the particle traversed. This knowledge of the hit location, as well as the information available in the signals themselves (like the total integrated charge and pulse height), will give us information on the trajectory, the velocity ( $\beta$ ), and the energy deposited by incoming and outgoing particles. The required timing resolution for the TOF detector is 400ps.

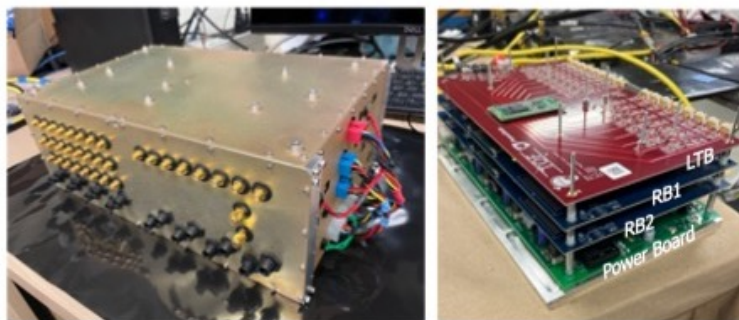


**Figure 5:** Readout and trigger box, closed (left) and partially disassembled (right) to show the electronics boards within.

#### 4. TOF Electronics

Figure 4 shows the signal pathway for trigger generation and data readout. Each SiPM preamp (two for each of the 160 paddles, for a total of 320 preamps) produces two copies of the signal: a low gain (LG) version and a high gain (HG) version. The LG signal is sent to a local trigger board (LTB), where it is passed through three discriminator levels. The three trigger levels are adjustable, and are currently set to 0.4 min-I (HIT), 2.5 min-I (BETA), and 30 min-I (VETO). HIT is intended to record all paddles with a track in them. BETA is intended to record paddles which have a slow-moving, high-ionizing track. VETO is intended to reject high-Z cosmic ray nuclei, such as Carbon and above. Each LTB encodes the signal from eight paddles using these three trigger levels, and sends a serialized data stream to the master trigger board (MTB) indicating the thresholds reached. There are 20 total LTBs, and the MTB takes the hit pattern from all 20 to make a trigger decision.

The tentative trigger decision requires both the correct energy deposition to trigger BETA but not VETO and a certain number of hits, of any level, in the outer and inner TOFs. If this trigger requirement is met, the MTB generates an event ID which allows for merging events between the TOF readout boards (RBs) and the tracker readout electronics. This event ID is then distributed, along with the trigger decision, to the two systems.

Each of the 40 RBs in the TOF receives eight HG waveform signal from the SiPM preamp and the trigger, event ID, and synchronized clock signal from the MTB. The RBs use the Domino Ring Sampler (DRS-4) ASIC, which samples at a rate of 2 GS/s to digitize a full 512 ns history of the waveforms.

There are 20 readout and trigger (RAT) boxes in the TOF; each RAT box has one LTB, two RBs, and a power board (PB) which accepts 24V battery power and provides power to the three other boards in the RAT box as well as the power and bias voltages to 16 SiPM preamps. See Figure 5 for photos of the inside and outside of the RAT boxes.

#### 5. Prototype and Testing

There have been three stages of prototyping and testing for the GAPS experiment. The first was the GAPS Functional Prototype (GFP) built at MIT Bates Lab in Boston Massachusetts during

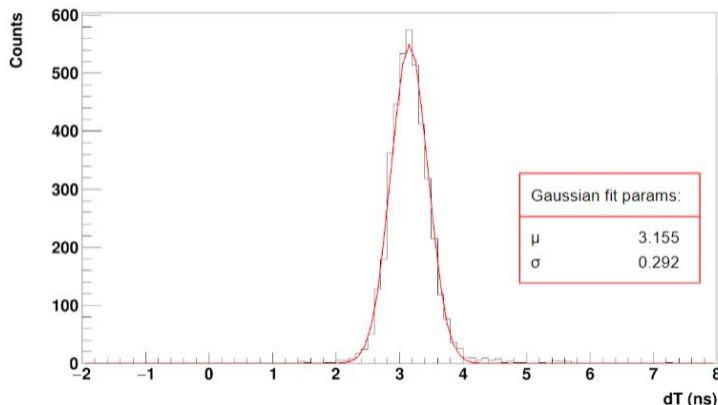


**Figure 6:** Distribution of times of flight for GFP data for which we find a timing resolution of 290ps based on a Gaussian fit.

the Fall of 2021. The GFP TOF was composed of two parallel panels of twelve 180 cm paddles, separated by a approximately a meter and placed over the GFP tracker. For GFP data taking, data from paddles directly on top of each other were read out using the same RB. Applying cuts on the time difference between paddle ends to select only vertical muons passing through the center of both the upper and lower paddles, it was possible to measure timing resolution performance (see Figure 6) to 290ps, which is significantly better than our requirement of 400ps. This is a significant validation for the design and a good test of hardware and readout systems.

The next phase of testing started in the fall of 2022, with the integration of the entire tracker with the inner TOF at the UC Berkeley Space Sciences Lab. This ground system testing also involved construction of the mechanical structure. Then, in June 2023, thermal and vacuum performance testing was done at National Technical Systems in El Segundo, CA. The TOF was operated for several hours at float pressure and at both the hottest and coldest temperatures expected in flight from the thermal model. During these operations, the TOF system performed as expected, with the electronic boards working correctly.

## 6. Conclusion and the Future of GAPS

At the time of this conference, it can be reported that the construction of the TOF components (electronics and hardware) is largely complete, that results from the GFP indicate that timing resolution goals are met, and that the TVAC testing was very successful. The TOF appears to be robust and prepared for a long-duration balloon launch.

GAPS is currently on schedule to launch during the austral summer of 2024-2025. During fall 2023, the payload will undergo further testing at Nevis Labs, Columbia University. In June of 2024, compatibility testing will be performed at NASA facilities in Palestine, TX, in preparation for shipment to Antarctica in the fall of 2024.

## References

- [1] Daniel Bauer, James Buckley, Matthew Cahill-Rowley, Randel Cotta, Alex Drlica-Wagner, Jonathan L. Feng, Stefan Funk, et al. Dark matter in the coming decade: Complementary paths to discovery and beyond. *Physics of the Dark Universe*, 7-8:16–23, mar 2015.
- [2] Fiorenza Donato. Antimatter from supersymmetric dark matter. In David B. Cline, editor, *Sources and Detection of Dark Matter and Dark Energy in the Universe*, pages 236–243, Berlin, Heidelberg, 2001. Springer Berlin Heidelberg.
- [3] Fiorenza Donato, Nicolao Fornengo, and Pierre Salati. Antideuterons as a signature of supersymmetric dark matter. *Physical Review D*, 62(4), jul 2000.
- [4] M. Aguilar, L. Ali Cavazonza, B. Alpat, G. Ambrosi, L. Arruda, N. Attig, S. Aupetit, et al. Antiproton flux, antiproton-to-proton flux ratio, and properties of elementary particle fluxes in primary cosmic rays measured with the alpha magnetic spectrometer on the international space station. *Phys. Rev. Lett.*, 117:091103, Aug 2016.
- [5] Jan Heisig, Michael Korsmeier, and Martin Wolfgang Winkler. Dark matter or correlated errors: Systematics of the AMS-02 antiproton excess. *Physical Review Research*, 2(4), oct 2020.
- [6] Rebecca K. Leane, Seodong Shin, Liang Yang, Govinda Adhikari, Haider Alhazmi, Tsuguo Aramaki, Daniel Baxter, et al. Snowmass2021 cosmic frontier white paper: Puzzling excesses in dark matter searches and how to resolve them, 2022.
- [7] R. Munini, E. Vannuccini, M. Boezio, P. von Doetinchem, C. Gerrity, A. Lenzi, N. Marcelli, S. Quinn, F. Rogers, J.L. Ryan, A. Stoessl, M. Xiao, N. Saffold, A. Tiberio, and M. Yamatani. The antinucleus annihilation reconstruction algorithm of the GAPS experiment. *Astroparticle Physics*, 133:102640, dec 2021.
- [8] Valentina Scotti, Alfonso Boiano, Lorenzo Fabris, Massimo Manghisoni, Giuseppe Osteria, Elisa Riceputi, Francesco Perfetto, Valerio Re, and Gianluigi Zampa. Front-end electronics for the gaps tracker, 2019.
- [9] Mengjiao Xiao, Achim Stoessl, Brandon Roach, Cory Gerrity, Ian Bouche, Gabriel Bridges, Philip Von Doetinchem, Charles J. Hailey, Derik Kraych, Anika Katt, Michael Law, Alexander Lowell, Evan Martinez, Kerstin Perez, Maggie Reed, Chelsea Rodriguez, Nathan Saffold, Ceaser Stringfield, Hershel Weiner, and Kelsey Yee. Large-scale detector testing for the gaps si(li) tracker. *IEEE Transactions on Nuclear Science*, pages 1–1, 2023.
- [10] H. Fuke, S. Okazaki, H. Ogawa, and Y. Miyazaki. Balloon flight demonstration of an oscillating heat pipe. *Journal of Astronomical Instrumentation*, 06(02):1740006, 2017.



**Full Authors List: GAPS Collaboration**

T. Aramaki<sup>1</sup>, M. Boezio<sup>2,3</sup>, S. E. Boggs<sup>4</sup>, V. Bonvicini<sup>2</sup>, G. Bridges<sup>5</sup>, D. Campana<sup>6</sup>, W. W. Craig<sup>7</sup>, P. von Doetinchem<sup>8</sup>, E. Everson<sup>9</sup>, L. Fabris<sup>10</sup>, S. Feldman<sup>9</sup>, H. Fuke<sup>11</sup>, F. Gahbauer<sup>5</sup>, C. Gerrity<sup>8</sup>, L. Ghisloti<sup>15,16</sup>, C. J. Hailey<sup>5</sup>, T. Hayashi<sup>5</sup>, A. Kawachi<sup>12</sup>, M. Kozai<sup>13</sup>, P. Lazzaroni<sup>15,16</sup>, M. Law<sup>5</sup>, A. Lenzi<sup>3</sup>, A. Lowell<sup>7</sup>, M. Manghisoni<sup>15,16</sup>, N. Marcelli<sup>18</sup>, K. Mizukoshi<sup>27</sup>, E. Mocchiutti<sup>2,3</sup>, B. Mochizuki<sup>7</sup>, S. A. I. Mognet<sup>19</sup>, K. Munakata<sup>20</sup>, R. Munini<sup>2,3</sup>, S. Okazaki<sup>27</sup>, J. Olson<sup>22</sup>, R. A. Ong<sup>9</sup>, G. Osteria<sup>6</sup>, K. Perez<sup>5</sup>, F. Peretto<sup>6</sup>, S. Quinn<sup>9</sup>, V. Re<sup>15,16</sup>, E. Riceputi<sup>15,16</sup>, B. Roach<sup>23</sup>, F. Rogers<sup>7</sup>, J. L. Ryan<sup>9</sup>, N. Saffold<sup>5</sup>, V. Scotti<sup>6,24</sup>, Y. Shimizu<sup>25</sup>, K. Shutt<sup>7</sup>, R. Sparvoli<sup>17,18</sup>, A. Stoessl<sup>8</sup>, A. Tiberio<sup>26,29</sup>, E. Vannuccini<sup>26</sup>, M. Xiao<sup>23</sup>, M. Yamatani<sup>11</sup>, K. Yee<sup>23</sup>, T. Yoshida<sup>11</sup>, G. Zampa<sup>2</sup>, J. Zeng<sup>1</sup>, and J. Zweerink<sup>9</sup>

<sup>1</sup>Northeastern University, 360 Huntington Avenue, Boston, MA 02115, USA <sup>2</sup>INFN, Sezione di Trieste, Padriciano 99, I-34149 Trieste, Italy <sup>3</sup>IFPU, Via Beirut 2, I-34014 Trieste, Italy <sup>4</sup>University of California, San Diego, 9500 Gilman Dr., La Jolla, CA 90037, USA <sup>5</sup>Columbia University, 550 West 120th St., New York, NY 10027, USA <sup>6</sup>INFN, Sezione di Napoli, Strada Comunale Cinthia, I-80126 Naples, Italy <sup>7</sup>Space Sciences Laboratory, University of California, Berkeley, 7 Gauss Way, Berkeley, CA 94720, USA <sup>8</sup>University of Hawai'i at Mānoa, 2505 Correa Road, Honolulu, Hawaii 96822, USA <sup>9</sup>University of California, Los Angeles, 475 Portola Plaza, Los Angeles, CA 90095, USA <sup>10</sup>Oak Ridge National Laboratory, 1 Bethel Valley Rd., Oak Ridge, TN 37831, USA <sup>11</sup>Institute of Space and Astronautical Science, Japan Aerospace Exploration Agency (ISAS/JAXA), Sagami-hara, Kanagawa 252-5210, Japan <sup>12</sup>Tokai University, Hiratsuka, Kanagawa 259-1292, Japan <sup>13</sup>Polar Environment Data Science Center, Joint Support-Center for Data Science Research, Research Organization of Information and Systems, (PEDSC, ROIS-DS), Tachikawa 190-0014, Japan <sup>15</sup>Università di Bergamo, Viale Marconi 5, I-24044 Dalmine (BG), Italy <sup>16</sup>INFN, Sezione di Pavia, Via Agostino Bassi 6, I-27100 Pavia, Italy <sup>17</sup>INFN, Sezione di Roma "Tor Vergata", Piazzale Aldo Moro 2, I-00133 Rome, Italy <sup>18</sup>Università di Roma "Tor Vergata", Via della Ricerca Scientifica, I-00133 Rome, Italy <sup>19</sup>Pennsylvania State University, 201 Old Main, University Park, PA 16802 USA <sup>20</sup>Shinshu University, Matsumoto, Nagano 390-8621, Japan <sup>22</sup>Heliospace Corporation, 2448 6th St., Berkeley, CA 94710, USA <sup>23</sup>Massachusetts Institute of Technology, 77 Massachusetts Ave., Cambridge, MA 02139, USA <sup>24</sup>Università di Napoli "Federico II", Corso Umberto I 40, I-80138 Naples, Italy <sup>25</sup>Kanagawa University, Yokohama, Kanagawa 221-8686, Japan <sup>26</sup>INFN, Sezione di Firenze, via Sansone 1, I-50019 Sesto Fiorentino, Florence, Italy <sup>27</sup>Research and Development Directorate, Japan Aerospace Exploration Agency (JAXA), 2-1-1 Sengen, Tsukuba 305-8505, Japan <sup>28</sup>Research and Development Directorate, Japan Aerospace Exploration Agency, Sagami-hara, Kanagawa 252-5210, Japan <sup>29</sup> INFN, Sezione di Firenze, via Sansone 1, I-50019 Sesto Fiorentino, Florence, Italy

This work is supported in the U.S. by the NASA APRA program (Grant Nos. NNX17AB44G, NNX17AB46G, and NNX17AB47G), in Japan by the JAXA/ISAS Small Science Program FY2017, and in Italy by Istituto Nazionale di Fisica Nucleare (INFN) and the Italian Space Agency (ASI) through the ASI INFN agreement No. 2018-22-HH.0: "Partecipazione italiana al GAPS - General AntiParticle Spectrometer." H. Fuke is supported by JSPS KAKENHI grants (JP17H01136, JP19H05198, and JP22H00147) and Mitsubishi Foundation Research Grant 2019-10038. The contributions of C. Gerrity are supported by NASA under award No. 80NSSC19K1425 of the Future Investigators in NASA Earth and Space Science and Technology (FINESST) program. R. A. Ong receives support from the UCLA Division of Physical Sciences. K. Perez and M. Xiao are supported by Heising-Simons award 2018-0766. Y. Shimizu receives support from JSPS KAKENHI grant JP20K04002 and Sumitomo Foundation Grant No. 180322. M. Yamatani receives support from JSPS KAKENHI grant JP22K14065. K. Yee is supported through the National Science Foundation Graduate Research Fellowship under grant 2141064. S. Feldman is supported through the National Science Foundation Graduate Research Fellowship under grant 2034835.